horticulturae

MDPI

Article

Smart Modular Vertical Farms: Addressing Food Security and Resource Efficiency in Singapore's Urban Environment

Chew Beng Soh [1,*], Barbara Ting Wei Ang [1], Yin Mei Fong [1], Szu-Cheng Chien [1], Hui An [1], Valentina Dessì [2], Matteo Clementi [2], Chuan Beng Tay [1], Michele D'Ostuni [3], Giorgio Gianquinto [3] and Francesco Orsini [3]

[1] Engineering Cluster, Singapore Institute of Technology, 1 Punggol Coast Road, Singapore 828608, Singapore
[2] Department of Architecture and Urban Studies, Politecnico di Milano, 20133 Milan, Italy; valentina.dessi@polimi.it (V.D.)
[3] Department of Agricultural and Food Sciences (DISTAL), University of Bologna, Viale Fanin, 44, 40127 Bologna, Italy; michele.dostuni@unibo.it (M.D.)
* Correspondence: chewbeng.soh@singaporetech.edu.sg

Abstract

This study presents a modular outdoor vertical farming system integrated into building façades to address urban food security and sustainability challenges in Singapore. The design integrates passive climate control, hydroponics and soil-based irrigation, with active monitoring of the vapor pressure deficit (VPD) and photosynthetically active radiation (PAR). Continuous visual imaging is used to support growth monitoring and predictive harvesting, reducing labor needs. Under experimental conditions, deployment of UCNP-coated light-conversion films improved crop yield by 30% and reduced plant heat stress. Photovoltaic arrays and battery storage enabled energy self-sufficiency and microclimate management in the modular farm. The results demonstrated that building-integrated vertical farms can enhance urban food resilience and resource efficiency, offering a scalable model for sustainable agriculture in land-constrained cities.

Keywords: vertical farming; hydroponics; vapor pressure deficit; sustainable agriculture; plant heat stress; crop yield

1. Introduction

Structural, economic and demographic changes have been driving up the urban population densities in South-East Asian cities. Just recently, Jakarta surpassed Tokyo as the most populous city globally [1]. Economic growth and rising demand for residential, commercial and industrials spaces have reduced the availability of agricultural land. Back in the 1960s, approximately 25% of Singapore's total land area was dedicated to agriculture. Singapore was entirely self-sufficient in poultry and eggs, while also producing 30–50% of its fish and vegetable needs. Currently, Singapore stands as a metropolitan city with only 1% of land area allocated for farming [2]. The COVID-19 pandemic in 2020 caused severe disruption of imports, emphasizing the importance of food security as a critical national priority [3]. Despite substantial effort towards supporting schemes for local agriculture, including the allocation and tendering of land space in Lim Chu Kang for farming activities, there has not been a corresponding increase in domestic crop production. Consequently, Singapore remains highly dependent on imports from neighboring countries like Malaysia, Vietnam and Indonesia [4]. Several initiatives were initiated to incorporate upcoming farming technologies in local farms. In recent years, vertical farming (VF) has been increasingly adopted as a land-efficient agricultural strategy in urban regions. Existing

Academic Editors: Silvio José Gumiere, Aikaterini Nikolaos Martini and Lamprini Tassoula

Received: 31 December 2025
Revised: 7 February 2026
Accepted: 24 February 2026
Published: 26 February 2026

VF systems typically rely on controlled-environment agriculture (CEA) facilities equipped with artificial lighting, active cooling, and IoT-based climate regulation to maintain optimal growth conditions for leafy greens and high-value crops. While these indoor farms achieve high productivity, their energy consumption for LED lighting, dehumidification, and air conditioning systems result in significant operational costs, limiting economic scalability. In Singapore, commercial VF initiatives deployed in the Lim Chu Kang and Neo Tiew areas demonstrate these trends, where moving gully hydroponics and sensor-driven greenhouse operations are used to boost yield, but at the expense of elevated electricity consumption. In parallel, Building-Integrated Agriculture (BIA) installations [5], including rooftop gardens and community-based farming on multi-story carparks, offer alternative pathways for distributed food production. However, these systems are mostly lacking in microclimate control and remain vulnerable to Singapore's intense solar heat load and humidity. Current outdoor VF and BIA models therefore face persistent challenges in managing heat stress, vapor pressure fluctuations, pest risks, and high labor demand. There are few companies with systems that integrate renewable energy, passive spectral modification, or automated growth monitoring into their farm setup.

However, several inherent challenges and concerns affect the expansion of these technologies. The naturally hot and humid climate in Singapore, which is currently suboptimal for crop cultivation, has been projected to intensify further over time. Plant heat stress is a significant challenge in Singapore's farming systems due to its hot, humid climate. Local greenhouses are constructed with common materials like polycarbonate or glass, which are prone to trapping heat, elevating internal temperatures beyond optimum thresholds for plant growth. Extensive concrete and glass surfaces in residential areas have further exacerbated the urban heat island (UHI) effect [4,6], contributing to increased temperatures in urban areas. These common building materials lack effective cooling mechanisms, allowing the temperatures of enclosed structures such as greenhouses or agricultural setups to reach 37 to 40 °C [7]. Consequently, the deployment of VFs in urban environments necessitates unique façade structure designs and materials that accommodate local climatic constraints. The next major challenge is the high domestic labor cost which demands cost-effective automation for day-to-day greenhouse operation [8]. The high startup capital expenditure is a strong deterring factor for setting up large-scale automated farms as the generated agricultural produce typically does not result in a return on investment. Most critically, the high domestic operational costs, including utility bills (electricity and water), increase the variable cost of production and make it challenging for local farmers to compete with imports. One potential strategy to minimize the operational cost is designing a structure that reduces the need for indoor cooling and artificial lighting.

In this work, a building-integrated, terrain-adaptable, modular farm design is demonstrated in an area with limited ground space. The modular farm also features automation functionalities like sensor-controlled ventilation and auto-dispensing of nutrients and water. A UCNP film frame was integrated into a modular farm for growth in a soil-based planter box unit to combat the challenges of plant heat stress. The research also utilizes continuous video imaging to monitor crop growth, allowing for the assessment of crop health and the determination of optimal harvesting times using the A-Frame farm unit structure. A photovoltaic array with integrated batteries installed on the roof and equipped with an inverter powers the ventilation fans and environmental (temperature, humidity) sensors in the farm. The research therefore addresses the design of the modular system and assesses its performances in terms of land use, labor and utility costs. While modular vertical farms and Building-Integrated Agriculture systems have been explored in Singapore, current solutions rely heavily on energy-intensive cooling or indoor controlled environments and often lack scalable microclimate control mechanisms that function outdoors. Existing

systems do not integrate spectral-conversion materials, renewable-powered environmental control, or automated computer-vision growth monitoring within a single modular façade structure. This work presents the first demonstration of an outdoor, building-integrated, terrain-adaptable modular farm that combines passive IR-mitigating UCNP films, off-grid PV-battery-powered ventilation, and depth-based visual imaging for predictive harvesting. These combined innovations address previously unresolved issues in heat stress, VPD fluctuations, operational energy costs, and labor intensity in urban modular farming systems.

2. Materials and Methods

2.1. Modular Farm Site and Structural Design

A terrace-stepped area at the back of the university campus (SIT@Dover, 10 Dover Road s139660, 1.310° N, 103.780° E) was chosen as the building site of the modular farm. This area was assessed and a 3D BIM design model (Autodesk Revit 2026 (v2026.3)/September 2025) was created, as presented in Figure 1a.

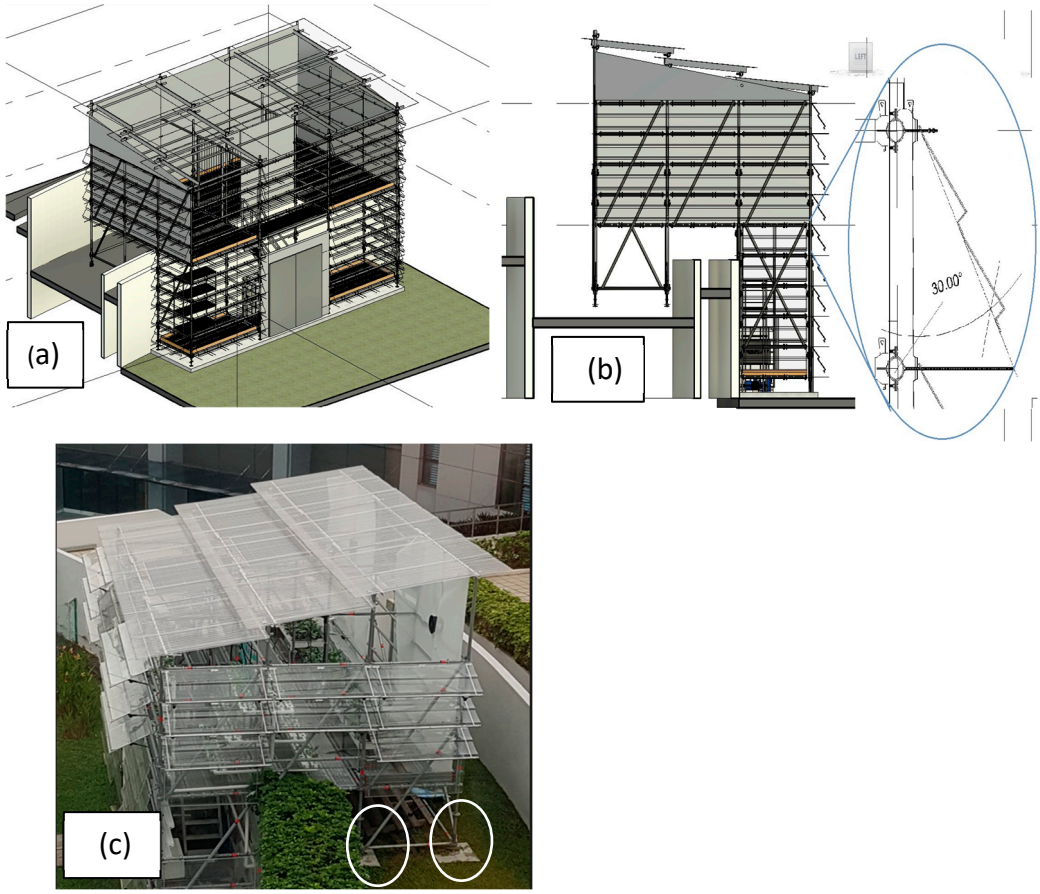

Figure 1. (**a**) 3D BIM model; (**b**) side view of the modular farm demonstrating the use of adjustable louvers to promote air ventilation, slope roof structures with 15 cm gaps between each tier to enable rainwater runoff, and use of a diffused corrugated roof structure to reduce glare and enable uniform diffused sunlight; and (**c**) actual structure constructed with scaffold base plate, base collar vertical support elements with concrete slab as circled and polycarbonate façade.

3D BIM modeling enabled the flexible customization of the modular parts, including various component elements such as the base collar, scaffolding poles and base plates. Each component element can be connected in the 3D model to create the modular farming structure. The base collar connects the mesh base plate with the vertical scaffold poles. The

scaffolding poles form the main frame of the modular farm and the base plate enables even load distribution by providing a flat weight-bearing surface. Concrete slabs (identified by circles in Figure 1c) support the base of the structure, spreading out the load to prevent the sinking of the vertical scaffold poles into the compacted soil (ground) [9].

Adjustable louvers allow the angle of the side-facade polycarbonate panels to be tilted to alter the volume of airflow in the enclosure. Prior work has reported on the tilt angle of the louvers at 25°, 45° and 60°, and ideal air velocities of 0.3 to 0.5 m/s were achieved at a height of 1.35 m from the floor level with a tilt angle of 45° [10]. Anemometers were installed to measure the airflow in the modular farm to keep the air regulation between 0.3 and 0.6 m/s by adjusting the tilt angle of the louvers. Airflow is important for healthy crop growth because it impacts heat transfer from the leaf, photosynthesis, and transpiration rates. In stagnant air, microclimates form around the plant, creating a layer of stationary air around the leaves. This boundary layer can slow the diffusion of gases into and out of the leaf. Stomata are pores where carbon dioxide enters the leaf for photosynthesis while water vapor exits through the process of transpiration. In semi-controlled environments such as modular greenhouses, proper airflow plays an important role in creating a physical environment that improves plant growth through increased heat dissipation, photosynthesis, and transpiration rates. As air flows past the surface of the leaf, the boundary layer is disrupted, enabling faster diffusion of heat and gases into and out of the leaf. This is ideal for leafy plant growth [11].

2.2. Planter Units and Irrigation Systems

To ensure the crops receive an adequate amount of solar irradiance, a Quantum Photosynthetically Active Radiation (PAR) meter (Apogee Instruments, Inc., Logan, UT, USA) was used for measurement of photosynthetic photon flux density (PPFD). In tropical climates like Singapore, day light integral (DLI) targets of 10 to 12.5 mol·m^2·d^{-1} at the plant's canopy can be easily achieved for most of the year [12]. The construction condition to achieve this ideal DLI range is to have the structure built facing either the east or west direction, enabling the crops to receive half a day of direct sunlight. The modular farm at SIT@Dover was built to fulfill this requirement. The concept of this modular farm is to demonstrate the ability to build an outdoor greenhouse without the need for energy-intensive cooling and the use of growth lights. Within the farm, PAR meters were placed at each unit of the A-Frames (AFU) and Suspended (SFU) planters to ensure that the crops receive an adequate amount of sunlight for a day, as shown in Figure 2.

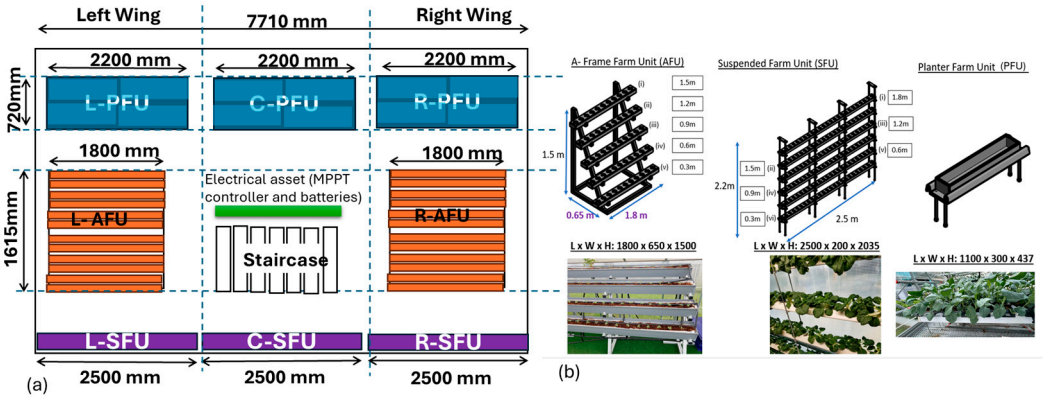

Figure 2. (**a**) 2D floor plan of the different types of planter layouts from the A-Frame, Suspended, and planter farm units using hydroponics for the first two and soil-based for the latter. (**b**) Pictorial drawing and images of the different types of planters ARU, SFU and PFU.

The AFU and SFU were irrigated by nutrient-film-technique (NFT) hydroponics, lowering the amount of water and nutrient supply needed. On the other hand, growth media (compost and cocopeat) was used for the planter farm unit (PFU) with nutrients delivered to the crops via drip irrigation. The nutrient circulation system was operated on an hourly on–off cycle. Intermittent operation also lowers energy consumption, extends pump lifespan, and lowers the frequency of preventive pump maintenance, extending the overall cost and operational efficiency (Figure 3).

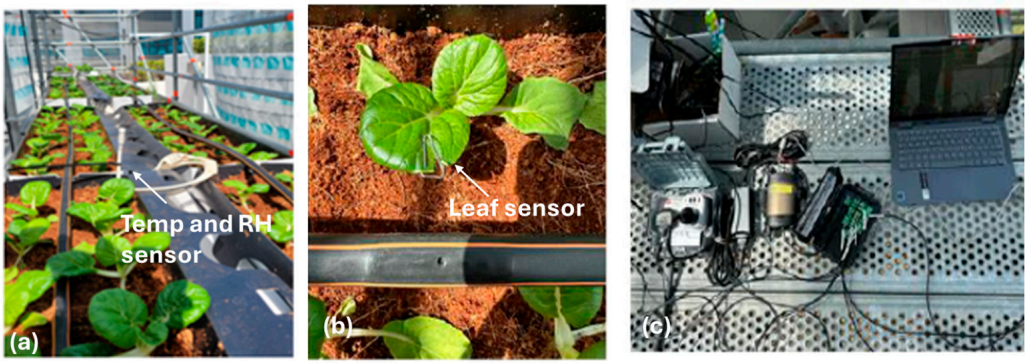

Figure 3. (**a**) Planter box position for growth of Pak Choi with sensor for detection of humidity and temperature in the enclosure. (**b**) Leaf sensors (thermistor) are used for measurement of the leaf surface temperature. (**c**) Data logger and controller setup.

2.3. Environmental Monitoring and Microclimate Measurement

The modular farm also includes a planter box setup equipped with HOBO MX1101 (Onset Computer Corporation, Bourne, MA, USA) temperature and humidity sensors to monitor the growing conditions. These measurements enable the calculation of the vapor pressure deficit (VPD), a key metric that combines air temperature and relative humidity (RH), while leaf surface temperature was recorded using a THERM-Micro Leaf Surface Temperature Measurement sensor (ICT International, Armidale, Australia). For the vapor pressure deficit (VPD) study, 15 Brassica Napa (Pak Choi) seedlings were transplanted into each planter box 14 days post germination and cultivated for a 28-day growth cycle. Each planter farm unit (PFU), as depicted in Figure 2, comprised four planter boxes, with each experimental cycle lasting approximately 28 days. The experimental setup included overhead frames above the planter boxes to evaluate the effects of the UCNP-coated film, uncoated film, and a control (no film) on plant heat stress mitigation and VPD optimization, as detailed in Section 3.1. It should be noted that the experimental design did not incorporate randomized switching of the film treatments among planter boxes, which is a limitation of the current methodology.

To assess how strongly the environment draws moisture from the plants, it is necessary to determine the difference between the plant's Saturated Vapor Pressure (which can be calculated from the leaf temperature) and the Vapor Pressure of the surrounding air ($V_{Psat} - V_{Pair}$).

The temperature of the saturated microclimate, T_{sat}, is measured from the surface of the plant leaf. To obtain V_{Psat}, Equation (1) is applied [12,13].

$$V_{Psat} = \frac{610.7 * 10^{\left(\frac{7.5T_{sat}}{237.3} + T_{sat}\right)}}{1000} \quad (1)$$

To get V_{Pair}, the temperature and humidity of the air are inputted into Equation (2). The integrated temperature and relative humidity sensors provide the T_{air} and RH values.

$$V_{Pair} = \frac{610.7 * 10^{(7.5T_{air}/237.3+T_{air})}}{1000} * \frac{RH}{100} \quad (2)$$

Therefore, the VPD can be found with the following equation:

$$VPD = V_{Psat} - V_{Pair} \quad (3)$$

2.4. Statistical Analysis

Statistical analyses were conducted to evaluate differences in crop growth and environmental parameters across experimental treatments. Fresh weight, canopy temperature, VPD values, and PPFD/DLI measurements were analyzed using parametric tests after confirming normality, and the data are reported as mean ± standard deviation (SD) in the results and discussion.

For the planter farm unit (PFU) experiments comparing UCNP film, blank film, and no-film conditions, differences in mean fresh weight were assessed using one-way analysis of variance (ANOVA) followed by Tukey's HSD post hoc test for pairwise comparisons. For the A-frame hydroponic system, comparisons between tiers (top, middle, bottom) and between left and right wings were evaluated using independent-samples *t*-tests or one-way ANOVA where appropriate. Statistical significance was set at $p < 0.05$.

Each PFU treatment included 15 plants per planter box, with four planter boxes per PFU. Two crop cycles were carried out for the study. For A-frame experiments, each tier included two gullies of 15 plants each and a mirror of a pair of gullies at each tier (total $n = 60$ plants per tier). Environmental sensor measurements (temperature, humidity, PPFD) were averaged over their sampling intervals and analyzed using repeated-measures ANOVA where applicable. Statistical analyses were performed using SPSS, (Version 30) and contour VPD maps were generated using Origin 2023b.

2.5. Ventilation Control with Renewable Energy System

High VPD has a negative effect on plant growth as it would induce high stomatal resistance and plant water stress (PWS). Accordingly, VPD should ideally be kept around 1.5 kPa [13]. One of the most common problems encountered when growing crops in enclosed environments like a greenhouse is the high humidity [14]. Moist environments provide a favorable condition for the development of various diseases, leading to significant reductions in product quality and quantity. Therefore, sufficient airflow is important in managing the humidity in the greenhouse. On the other extreme, heatwaves or dry spells in the period between mid-June and August can result in a deficiency in moisture in greenhouses. Hence, it is crucial to have good air circulation in the outdoor modular farm for consistent crop yield across the year by installing ventilation fans. To lower the utility cost, PV with battery storage is integrated into the farm. The PV system is equipped with a Maximum Power Point Tracking (MPPT) controller to regulate the captured solar irradiance and to store excess energy in the lithium-ion batteries. The power inverter is necessary to convert the DC to AC to power the ventilation fan.

2.6. Depth-Imaging System for Crop Monitoring

In the farming system, it is important to avoid over-maturation of crops, as prolonged growth leads to continued nutrient uptake from the hydroponic solution and can result in increased bitterness in leafy greens. Timely harvesting, therefore, ensures both higher economic returns for farm operators and improved palatability for consumers. To support this objective, two depth-sensing Luxonis OAK-D cameras (Luxonis, Westminster, CO,

USA) were integrated with Raspberry Pi 3B microprocessors and were deployed on each A-frame structure, as shown in Figure 4. One camera (Figure 4a) was installed at a vertical distance of 66 cm and a horizontal distance of 98 cm away from the canopy of the Pak Choi plants, and the other (Figure 4b) was at the canopy height and at a horizontal distance of 98 cm away from the AFU. Farm-wide Wi-Fi connectivity enabled data collection and the transmission of alert notifications, while system power was supplied by a solar-powered battery source.

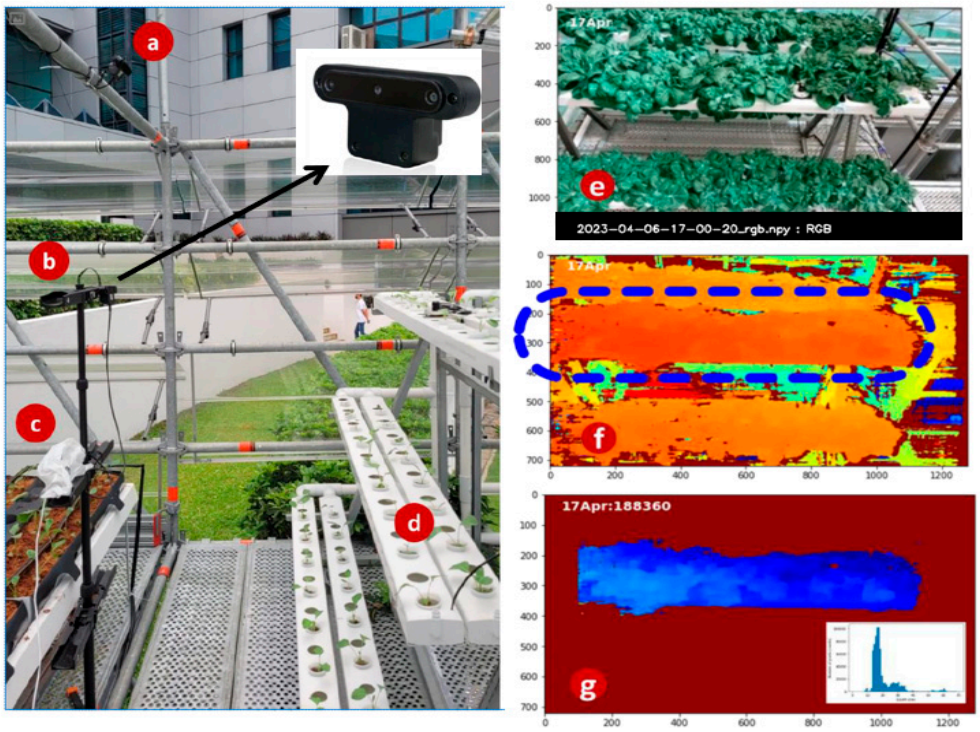

Figure 4. Deployment of (**a**) top and (**b**) front depth cameras (as shown in inset) connected to (**c**) microprocessor boards. Both cameras monitor the (**d**) A-frame planter with young seedlings (of Pak Choi) on Day 3. (**e**) A color image of Pak Choi (at Day 20) a with (**f**) its depth information enables a quick and efficient selection of the blue dotted region for (**g**) segmentation of the image and depth profile of the gullies for further analysis.

The selected components used were lightweight, robust, and easily mounted on scaffold poles, demonstrating the practicality and scalability of the deployment. Data were collected across multiple crop growth and harvest cycles. Camera height and orientation were carefully adjusted to capture all planters within the field of view while maintaining alignment along the vertical center of the rack. Color, stereo, and depth-disparity data were continuously captured and stored locally on the Raspberry Pi. Images were saved in NumPy array format to improve processing efficiency and reduce storage requirements. The complete image dataset was retained to support subsequent data analysis and model development across the harvesting cycle of the farm.

The depth sensor data provided multiple imaging modes that were combined for analysis in this study. By identifying the spatial position of each planter within the captured images and estimating the corresponding camera-to-object distance, individual planters were accurately segmented for subsequent analysis. To improve frame capture rates, image processing was decoupled from data acquisition. Snapshots of color (RGB), stereo (mono-left and mono-right), and depth disparity data were acquired, with each image labeled by date, time, and source to provide contextual reference (Figure 4g).

The AFU has three tiers, top, middle and bottom, at a vertical spacing of 50 cm. Each tier has two gullies with 15 planter units per gully. Two batches of Pak Choi growth were grown on the AFU between (i) early February and early March and between (ii) late March and late April and are reported in this work. The young seedlings were transferred two weeks after germination to the AFU and grown by the NFT. The DLI was calculated by integrating the measured PPFD over the photoperiod, defined as the duration where t1 and t2 define the time boundaries of daylight hours in a day. The DLI was computed using Equation (4).

$$DLI = 3600 \times 10^{-6} \int_{t1}^{t2} PPFD\, dt \quad (4)$$

3. Results and Discussion

Lab-fabricated light-conversion (UCNP) films were used to mitigate the direct heat gain and manipulate the growth environment to achieve optimal PPFD and temperature during the plant's active photosynthetic time, as reported in previously published work [15], and the growth result for the average growth cycle is reported in Section 3.1. In addition, energy utilization within the farming system was evaluated. Photovoltaic (PV) panels were integrated into the farm system, providing a source for the energy enhancement needed to achieve net-zero energy farming as reported in Section 3.2. As the PV system generates electrical energy in the form of direct current (DC), an inverter is required to convert the harvested energy into alternating current (AC) suitable for powering the equipment in the farm. Finally, the implementation and application of video analytics for continuous monitoring of the plant growth in the farming setup are discussed in Section 3.3.

3.1. Growth of Pak Choi with Overhead UCNP Film Frame

Farmers in Singapore use high-tech, land-efficient setups like vertical farms and hydroponics in controlled-environment greenhouses that include growth LEDs and sophisticated IoT systems. There are also some soil-based farms that employ all-encompassing netting for pest prevention. However, trapped heat remains a persistent issue. Farmers attempt to mitigate the heat by energy-intensive methods using air conditioning, chillers, and cooling pads, which increases their operating costs exponentially. In this section, we mitigate crop heat stress with passive intgeration of the overhead UCNP film frame for planter farm unit growth for Pak Choi.

3.1.1. Deployment of UCNP Film Frames into Modular Farm

Figure 5a shows the histogram plot of the average fresh weight of the Pak Choi and at the various PFUs. The average fresh weight for the L-PFU, C-PFU and R-PFU was 68.71 ± 6.37 g, 54.40 ± 9.15 g and 46.78 ± 14.58 g, respectively. Figure 5b–d show the L-PFU with an overhead frame installed with the UCNP film, the R-PFU with no film acting as the control sample, and the C-PFU with an overhead frame installed with a blank film. A schematic of the setup is shown in Figure 5e.

The UCNP film is mounted onto an aluminum frame to enable its deployment over the PFU setup. The light conversion film was customized to convert non-usable infrared light (IR) into red visible light for better photosynthesis in the plants [15]. For a tropical climate like in Singapore, there is strong solar irradiance in the infrared regime between 0.9 μm and 3 μm, which can lead to higher greenhouse temperatures. The film attempts to reduce this phenomenon. The results in Figure 5a show that the average yield for Pak Choi in the L-PFU is higher than those of both the C-PFU and R-PFU. This shows that the light conversion film contributes to the enhanced growth of the crops.

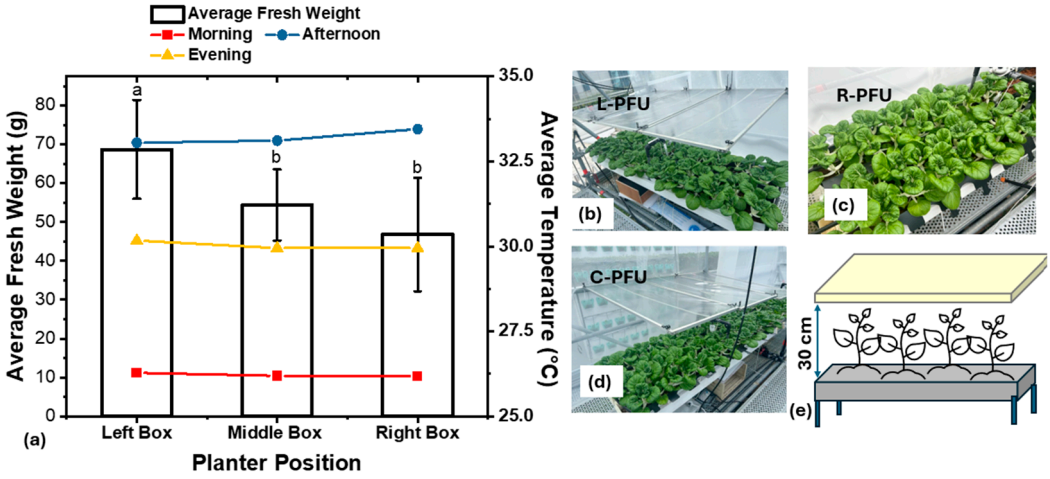

Figure 5. (**a**) Average fresh weight of Pak Choi grown in the left PFU (UCNP-coated film), center PFU (blank film), and right PFU (no film). Data are presented as mean ± SD (n = 60 plants per PFU). Statistical differences among treatments were assessed using one-way ANOVA, followed by Tukey's HSD post hoc test. Different letters above the bars indicate statistically significant differences at $p < 0.05$. Canopy-level temperature differences recorded during the growth period are shown alongside yield data. (**b**–**d**) Photographs of PFU configurations for growth of Pak Choi on the planter farm units. (**e**) Schematic of PFU setup with overhead frames.

The mean temperatures during the specified intervals, morning (10:00–11:00), afternoon (12:00–13:00), and evening (16:00–17:00), were continuously monitored using sensors positioned at the crop canopy level for the three PFUs setup for the growth cycles. The resulting data are presented in Figure 5a. There is a decrease of 1.0 °C in the average temperature between the R-PFU and the L-PFU, indicating that the light conversion film has reduced the IR transmittance to the planter box. The corresponding increase in yield of the Pak Choi in the L-PFU implies that some of the IR light has been converted to red light, contributing to an increased plant growth rate. While the overhead blank film also provides a reduction in the heat transmitted, and better yield, there is a 7.7% increase in yield with the addition of the light conversion material on the L-PFU. Overall, the Pak Choi in the L-PFU has a 30% increase in yield as compared to the control in the R-PFU.

3.1.2. VPD at the Modular Farm with Different Film Frames

Understanding crop physiology in relation to the vapor pressure deficit (VPD) is essential for optimizing growth conditions within the microclimate of the modular farm. Singapore often experiences extreme weather conditions such as prolonged dry spells between May and August, followed by intense rainfall during the monsoon season. These weather changes can adversely affect crop yields over the year. This poses a challenge to microclimate control due to the constant changing ambient conditions. However, maintaining VPD within an optimal range is critical for healthy plant development. When the VPD is too low, typically associated with humidity levels approaching 100%, plants struggle to transport nutrients efficiently to the leaves. This condition impairs water movement within the plant, resulting in physiological stress. Conversely, excessively high VPD during dry weather forces plants to transpire at elevated rates, leading to increased water loss through the stomata. If the root system or water supply cannot compensate for this loss, plants may wilt as the rate of water uptake falls short of demand. Both extremes of low and high VPD negatively impact crop health and productivity, highlighting the importance of precise environmental control in vertical farming systems [16].

Optimal development of leafy greens is achieved when VPD is maintained within the range of 0.8 to 1.2 kPa, particularly during the mature growth stage [17,18]. Over the 28-day growth cycle, the VPD contour map was generated for different permutations of temperature versus relative humidity using Equations (1)–(3). This captures the dynamic microclimate conditions experienced by the crops during their growth cycle. By calculating the VPD values across different combinations of humidity and temperature, we produced 2D contour maps (Figure 6a–c) for each PFU. These maps feature a circled red region that highlights the optimal VPD range. For the growth of Pak Choi in the PFUs, the peak temperature attained (based on the VPD plots) for R-PFU (Figure 6a) and the C-PFU is 36.5 °C (Figure 6b), while L-PFU (Figure 6c) reaches 37 °C. The datapoints above 36 °C are much lower for L-PFU as compared to C-PFU and R-PFU (as shown by the area above the black dashed lines) in Figure 6a–c. The measurement of the temperature is carried out with the THERM-Micro Leaf Surface Temperature Measurement sensor mounted at the surface of the leaves for the crops. Notably, in Figure 6a, the L-PFU displays the largest area within this optimal zone, indicating more favorable conditions for crop growth when an overhead UCNP film frame is mounted 30 cm above the planter bed.

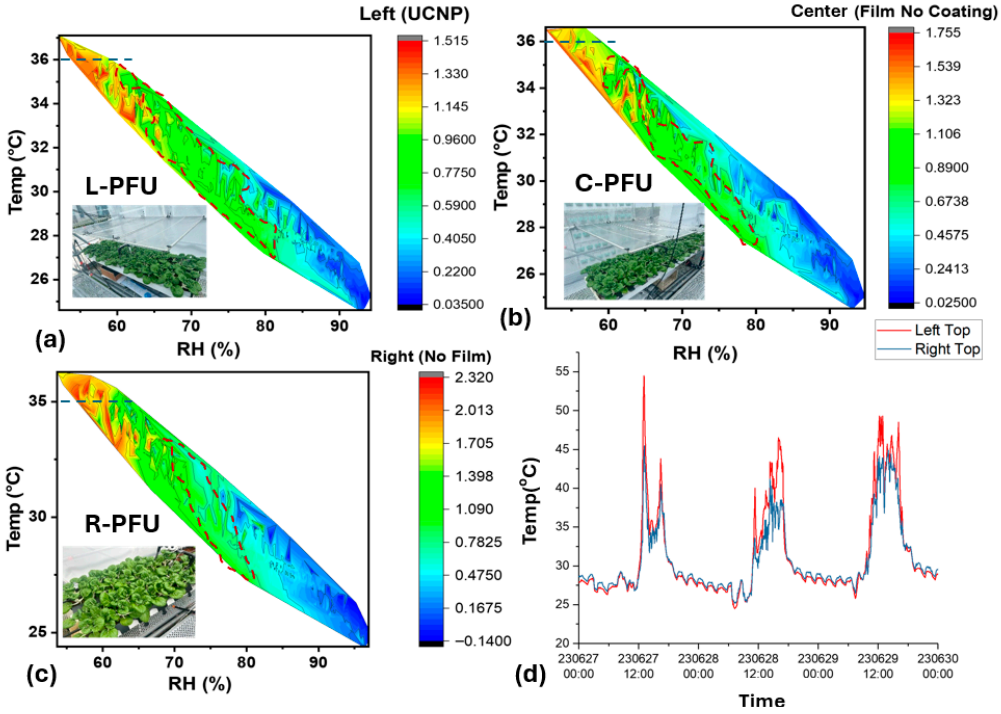

Figure 6. Plot of VPD for the (**a**) left planter (with UNCP film), (**b**) center planter (non-coated film), and (**c**) right planter (no film), and the (**d**) temperature difference at two ends (the left and right) of the structure.

Figure 6d illustrates an approximately 3 °C to 5 °C higher ambient temperature difference for the left wing as compared to the right wings of the modular farm across 3 days, as measured by roof-mounted temperature sensors. Despite this disparity in the ambient conditions, the temperature variation among the three PFUs was minimal, with the L-PFU (with overhead UCNP film) only registering a maximum temperature 0.5 °C higher than that of the control R-PFU. This indicates effective heat shielding of UCNP and consequently lowering the expected higher leaf surface temperatures for L-PFU since the temperature difference is 3 °C or more from the roof-mounted sensors. This demonstrates the significance of the UCNP film's contribution to heat mitigation in the modular farm. Correspondingly, the maximum VPD values decreased from 2.32 kPa in the R-PFU (control)

to 1.788 kPa in the C-PFU and 1.515 kPa in the UCNP-covered L-PFU, bringing climatic conditions closer to the optimal range of 0.8 to 1.2 kPa.

3.2. Photovoltaics (PV) and Battery Integration for Self-Sustaining Ventilation and Misting System

To regulate the airflow in the modular farm, two exhaust fans are installed. Each fan has a rotational speed of 2550 RPM and an air flow of 0.566 m^3/s. The fans use a single-phase 220/230 VAC (50 Hz) motor with an operation current of 0.6 A and power of 136 W. Two 1 m × 2 m photovoltaic (PV) panels are mounted on the roof of the modular farm 2.5 m above the planter units. Considering that the monocrystalline panel has an average efficiency of η = 20% and an irradiance of G = 1000 W/m^2 with an area of 2 m^2, the rated power output per PV panel is about 400 W using Equation (5).

$$P = G \times A \times h \quad (5)$$

The daily energy output depends on the amount of available sunlight, typically measured as peak sun hours (taken to be about 5 h as Singapore lies in the equatorial region). The energy generated for each panel is approximately 2.0 kWh per day on average and 4.0 kWh in total with two panels to form a PV array. Batteries are employed to store excess energy that can make up for the energy needs during non-peak hours (Figure 7).

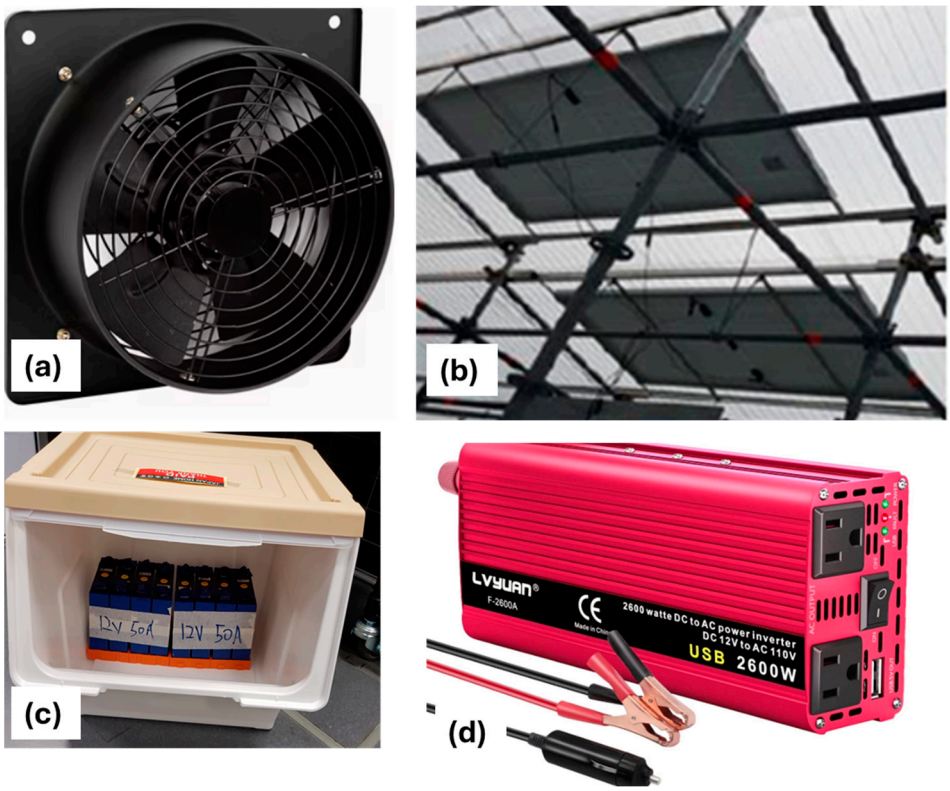

Figure 7. PV-powered ventilation system with (**a**) exhaust fans, (**b**) 1 m-by-2 m PV panels mounted on roof with an MPPT charge controller, (**c**) lithium-ion batteries, and (**d**) power inverters.

The single line diagram shared on the electrical asset is shown in Figure 8. The monocrystalline PV array generates 4.0 kWh @ 48 V nominal (approx.) and hence the DC per array ≈ 4000 W ÷ 48 V = 83 A (approximate). Given the need for conservative design margins in photovoltaic short-circuit current and MPPT ratings, the selected controller must be capable of handling continuous currents exceeding 83 A while providing an adequate open-circuit voltage (Voc) margin. Accordingly, the Victron SmartSolar MPPT 150/100,

rated for a 100 A output current and a maximum Voc of 150 V, was selected for this system. This configuration ensures that the PV system can reliably operate within safe limits while effectively harvesting solar energy at its maximum power point. For the battery bank, a 48 V, 100 Ah battery array was selected to balance practical deployment considerations as in Singapore, due to passing cloud cover, solar irradiance fluctuates with time and the dynamic power harnessed by PV fluctuates with time. As shown in the line diagram in Figure 8, the power from the PV is used to charge the batteries instead. This configuration provides a nominal capacity of approximately 4.8 kWh, with an estimated usable capacity of 3.84 kWh at 80% depth of discharge (DoD), offering sufficient operational headroom and providing constant power to the two ventilation fans. Lithium iron phosphate ($LiFePO_4$) chemistry was chosen due to its suitability for deep-cycle operation and enhanced thermal stability for the intended application.

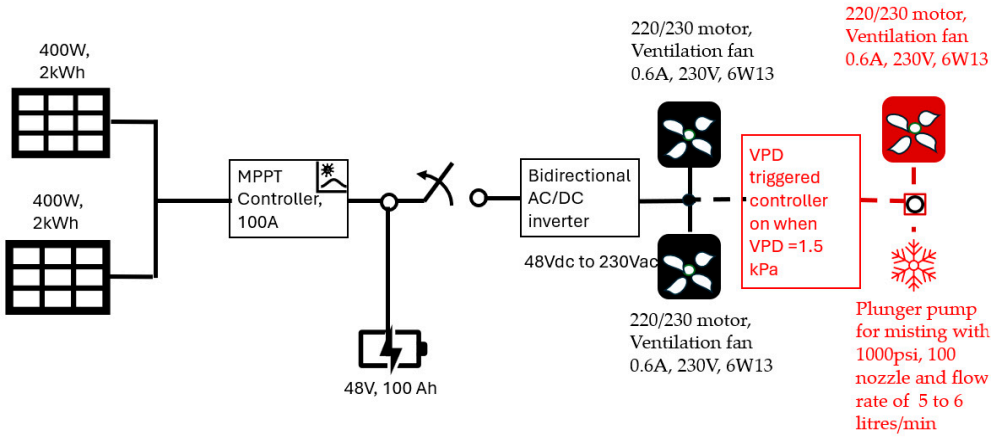

Figure 8. Single line diagram for the setup of the solar-powered ventilation system with the rating for each component. The red labeled diagram is the addition system that can be included to lower the VPD with the excess energy stored in the battery.

As such, the system operates two ventilation fans controlled by a timer between 11:00 and 17:00 to mitigate elevated midday temperatures. The average power consumed by the fan is $P_{fan} = I \prime V = 0.6\ \text{A} \prime 230\ \text{V} = 138\ \text{W}$. Over approximately six hours of daily operation, the ventilation system which comprises two fans will demand a total of $E = 2 \times P_{fan} \times t = 1.656$ kWh of energy. With consideration of a total of 4.0 kWh of power generated from the PV array and an estimated usable capacity of 3.84 kWh at 80% depth of discharge (DoD) of the battery, this is more than sufficient to operate the ventilation fan system. As the electrical system operates independently of the grid, surplus energy can be utilized to activate additional ventilation fans in response to increased cooling demand, as illustrated in Figure 8.

Based on the above results, this study proposes a data-driven approach to microclimate control in which existing vapor pressure deficit (VPD) mapping results (Figure 6), derived from combinations of leaf surface temperature and ambient humidity, can be used to control ventilation and misting systems. Based on predefined VPD thresholds, a ventilation fan can be activated to enhance airflow, while misting can be selectively deployed during hot and dry conditions to increase relative humidity and reduce VPD. Both the ventilation fan and misting pump can be powered by renewable energy stored in the battery system. For large-scale misting configurations (e.g., 100 nozzles), a high-pressure plunger pump capable of delivering approximately 4–5.5 L min^{-1} at pressures of 800 psi or higher is suitable to achieve fine atomization, enabling rapid evaporative cooling without wetting plant surfaces. Given that misting is required only intermittently (typically less than 3 min per activation), the associated daily energy demand remains low. Collectively, this

framework demonstrates the potential to leverage existing environmental data to fine-tune greenhouse microclimate control and maintain VPD within optimal ranges for crop growth.

3.3. A-Frame Structure for Hydroponic Growth of Leafy Greens in the Left and Right Wings of the Modular Farm

One of the key challenges associated with managing multiple small-scale vertical farms distributed across the island is the limited availability of manpower and resources for continuous monitoring of crop growth conditions. A potential solution lies in the adoption of continuous video monitoring and automation to enable remote supervision and reduce labor demands.

3.3.1. Impact of DLI and Temperature on Average Fresh Weight of Leafy Greens for A-Frame Planter Unit

The first two cultivation batches focused on Pak Choi, with the objective of establishing a benchmark comparison of crop growth between the left and right wings of the modular farm. This comparative study evaluated the relative performance of crops under differing microclimatic conditions. The A-frame configuration was adopted to enhance solar irradiance exposure across multiple vertical levels compared with the vertically suspended planter system (Figure 2a).

Each A-frame has a total of twelve gullies, with two positioned on each side of the frame at each tier (Figure 9a). Analysis of average fresh weight across tiers indicated that crops grown on the top tier exhibited significantly higher biomass, with increases of approximately 36% and 70% relative to the middle and lower tiers, respectively (Figure 9b). This is attributed to the closer proximity of the top tier to the roof and its likelihood of less shading and higher DLI as compared to the middle and lower tiers. The temperature does not have any effect on the different tiers at the same time of day. Similarly, the average number of leaves per plant was comparable across all tiers, ranging from approximately 10 to 11 leaves per Pak Choi plant.

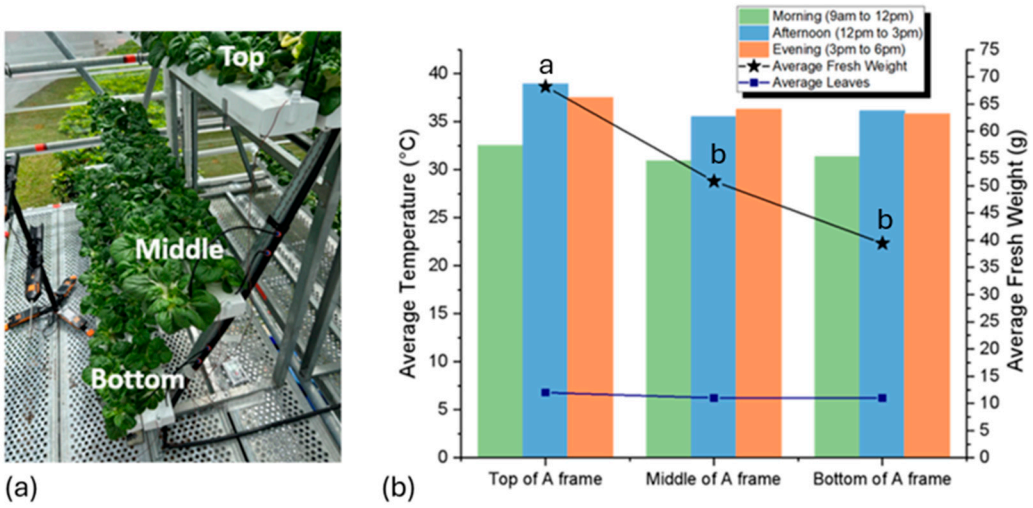

Figure 9. (**a**) Photograph of the A-Frame hydroponic unit (AFU). (**b**) Average fresh weight of Pak Choi harvested from the top, middle, and bottom tiers of the A-Frame. Data are expressed as mean ± SD (n = 30 plants per tier). Statistical comparisons were performed using one-way ANOVA with Tukey's post hoc test. Data not sharing the same letter differ significantly ($p < 0.05$). Different letters indicate groupings based on one-way ANOVA with Tukey's HSD post hoc comparison ($\alpha = 0.05$) for average fresh weight.

Crop growth over the entire harvest cycle was monitored for planter gullies mounted on the A-frame structures. For analytical clarity, the A-frame was subdivided into the upper, middle, and lower tiers, with the upper tier on the left wing denoted as L upper, as labeled in Figure 10a. At harvest, the average fresh weight of crops grown on the upper tier of the left wing was 86 g, compared to 68 g on the corresponding upper tier of the right wing. These results corroborate findings from both batches of the growth study, demonstrating a strong correlation between average fresh weight and the daily light integral (DLI) received by the crops. The higher DLI measured on the left wing relative to the right wing contributed to an approximate 20% increase in yield, as indicated by fresh biomass. Photosynthetic photon flux density (PPFD) sensors were used to quantify the instantaneous availability of photosynthetically active radiation (PAR) in the 400–700 nm wavelength range, which is critical for photosynthesis.

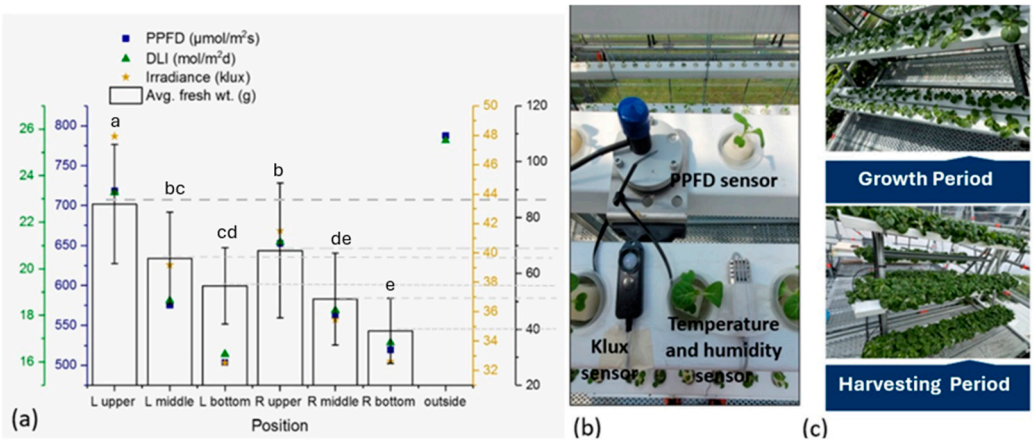

Figure 10. (**a**) Relationship between photosynthetic photon flux density (PPFD), daily light integral (DLI), solar irradiance, and average fresh weight of Pak Choi grown on the upper, middle, and lower tiers of the A-frame planter unit. Values represent mean measurements ± standard deviation (SD) averaged across plants within each tier (n = 60 plants per tier). Fresh weight values correspond to harvest measurements from the same cultivation cycle. (**b**) Sensor placement for PPFD, lux, and temperature/relative humidity measurements. (**c**) Growth phase and harvest images. Different letters above the bars indicate statistically significant differences at $p < 0.05$.

Photosynthetic photon flux density (PPFD) and solar irradiance were measured using a PAR meter and a lux sensor, respectively, together with temperature and relative humidity sensors. All measurements were logged using a data acquisition system and transmitted to a cloud-based platform for storage and analysis. The placement of the sensors is illustrated in Figure 10b. Crop growth on the A-frame structure was documented, corresponding to the growth and harvest stages, during the period from late March to late April.

During the crop growth study, it was noted that there were slight differences in the lighting conditions in the left and right wings of the modular farm. Solar irradiance spans a broad spectral range from ultraviolet (UV) to far-infrared wavelengths [19]; however, crop growth primarily relies on visible light, particularly red and blue wavelengths, with only minimal UV exposure required to support healthy development and photosynthesis [20,21]. As the modular farm operates as an enclosed outdoor system utilizing natural sunlight as the primary light source, it is essential to monitor and mitigate undesirable solar heat gain to prevent excessive thermal accumulation within the enclosure. Observations indicate that during the morning and afternoon periods, temperatures at the bottom tier were slightly higher than those at the middle tier. This

temperature elevation can be attributed to radiative heat emission from the metal grating scaffold planks.

3.3.2. Implementation of Visual Imaging for Predictive Harvesting Time for Leafy Greens

As shown in Figure 11a, depth measurements enabled estimation of foliage height (y) at each point along the planters. Integration of these height profiles across individual planters allowed the calculation and temporal tracking of foliage volume for each tier. Figure 11c presents the normalized daily foliage density over the growth cycle. The representative color and depth images are collected (as illustrated in Figure 11d). The resulting growth profiles exhibit an initial post-transplantation lag phase, followed by a linear growth period and a plateau corresponding to crop maturity. The normalized foliage volume shows an increasing trend with a dip on 19 April (Figure 11b). Closer examination shows that the removal of a pot was the cause of the dip, which testifies to the sensitivity of the technique for monitoring growth (Figure 11c). The reduction in the normalized foliage volume on 19 April was registered where the plant was taken out (due to pest outbreak). This methodology supports timely harvest and optimizes harvest yield by enabling continuous, real-time monitoring of crop growth dynamics. With the segmented depth area images, this allows the normalized foliage volume to be estimated and plotted in Figure 11b.

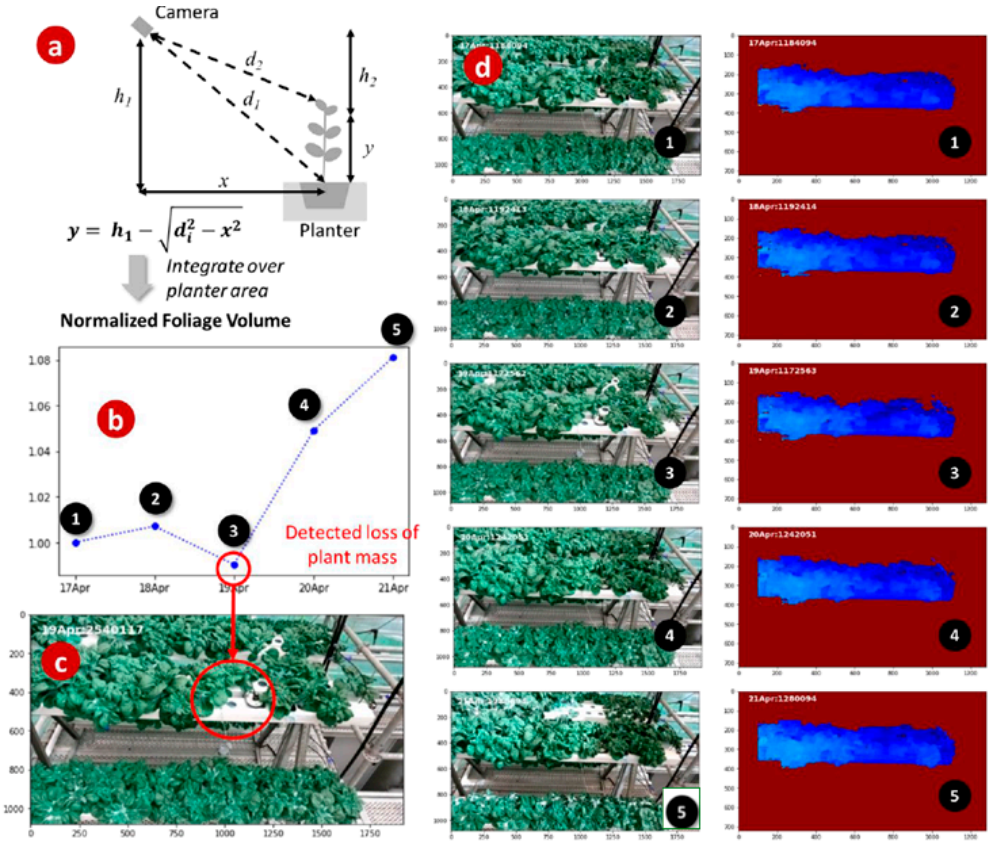

Figure 11. (**a**) Estimating foliage height and volume from depth data. (**b**) Chart showing the normalized plot of daily foliage volume over one week. (**c**) The drop in foliage volume on Day 3 is due to the removal of a pot of plant. (**d**) The points (1), (2), (3), (4) and (5) correspond to the color and depth images.

The integration of visual imaging technologies to predict the optimal harvesting time for leafy greens has the potential to substantially reduce the manpower required for routine crop monitoring. A farm technologist can use the image sent from the visual

imaging system to identify potential pest issues and reduce the need for regular random checks on the modular farm distributed in the urban residential areas. This will reduce the manpower demand and can enhance the overall productivity of the farm. It can also lower operational costs for farm operators in terms of transport to and from the distributed modular farms. The cost tabulation is as provided in Table 1. Based on these assumptions, the comparative cost model indicates that the automated imaging system achieves payback of the fixed capital cost within approximately seven months. This calculation considers the displacement of recurring manual inspection expenses by a one-time capital investment, alongside minor operational energy overheads. The system thereby enhances long-term cost efficiency while enabling higher-frequency, real-time monitoring without additional manpower requirements. Such advancements are particularly critical for modular farms deployed within satellite residential estates, where workforce and space constraints are often more pronounced. Moreover, the use of predictive imaging supports healthier crop development and facilitates more systematic and effective harvesting and replanting cycles, ultimately contributing to more sustainable and resilient farm management practices.

Table 1. Cost structure for using conventional manpower as compared to integration of visual imaging technologies.

Method	Conventional Manpower	Integration of Visual Imaging Technologies
Fixed cost	0	$2000 for 4 set of cameras
Variable cost	$300 per month	$5 per month for utility

4. Conclusions

This study presents a pioneering integration of passive spectral management, renewable energy-driven microclimate control, and automated visual analytics into a modular vertical farming system designed for outdoor deployment on building façades. By combining adjustable polycarbonate louvers, hydroponics and soil-based systems, and environmental sensing, the system demonstrates that stable crop growing conditions can be achieved without energy-intensive cooling or artificial lighting. Field results show that UCNP light conversion films substantially reduce heat load and improve crop yield by approximately 30%, while VPD regulation enabled by PV-powered ventilation maintains microclimate conditions closer to the optimal range for leafy greens.

The system's off-grid PV battery architecture ensures reliable operation of ventilation and potential misting functions, even under Singapore's fluctuating irradiance and weather patterns, thereby lowering operational utility costs and enhancing deployment scalability. The integration of depth-based visual imaging further provides real-time crop growth assessment and predictive harvesting, reducing reliance on manual monitoring, which is a critical advantage for distributed modular farms situated across residential or commercial estates.

The key novelty of this work lies in the holistic integration of these technologies into a single, terrain-adaptable modular farm that functions effectively in an outdoor tropical environment. Unlike existing VF or BIA models, which depend on artificial climate control or centralized manpower, this system emphasizes energy autonomy, heat-stress mitigation, and labor efficiency. Together, these advancements offer a new paradigm for urban agriculture in dense cities, enabling scalable, sustainable, and resilient food production systems. Further work could focus on randomized experimental design, expanded crop testing, and long-term operational cost–benefit validation across multiple deployment sites.

Author Contributions: Conceptualization, C.B.S., V.D. and S.-C.C.; methodology, C.B.S. and B.T.W.A.; software, C.B.T.; validation, B.T.W.A., C.B.T. and C.B.S.; formal analysis, H.A., C.B.S., B.T.W.A. and M.D.; investigation, H.A., Y.M.F., G.G. and B.T.W.A.; resources, B.T.W.A., G.G. and Y.M.F.; data curation, C.B.S., B.T.W.A., Y.M.F. and C.B.T.; writing—original draft preparation, C.B.S. and B.T.W.A.; writing—review and editing, B.T.W.A. and F.O.; visualization, B.T.W.A. and C.B.T.; supervision, H.A., M.C. and M.D.; project administration, C.B.S., V.D., F.O. and M.C.; funding acquisition, C.B.S. and V.D. All authors have read and agreed to the published version of the manuscript.

Funding: The authors acknowledge the funding support by the (i) Italy Singapore Science and Technology Cooperation, Grant Number R23I0IR035, and (ii) the Singapore Food Story (SFS) R&D Programme first Grant Call (Theme 1 Sustainable Urban Food Production) Award SFS_RND_SUFP_001_09.

Data Availability Statement: The original contributions presented in this study are included in the article. Further inquiries can be directed to the corresponding author.

Conflicts of Interest: The authors declare no conflict of interest.

References

1. United Nations. *World Urbanization Prospects 2025: Summary of Results*; UN DESA/POP/2025/TR/ NO. 12; United Nations: New York, NY, USA, 2025.
2. Fujii, T.; Waibel, C.; Du, X.; Shi, Z. *Food Self-Sufficiency and Building-Integrated Urban Agriculture: Lessons from Singapore*; SMU Economics and Statistics: Singapore, 2025; p. 22.
3. Tortajada, C.; Lim, N.S.W. Food Security and COVID-19: Impacts and Resilience in Singapore. *Front. Sustain. Food Syst.* **2021**, *5*, 740780. [CrossRef]
4. Mughal, M.O.; Li, X.-X.; Norford, L.K. Urban heat island mitigation in Singapore: Evaluation using WRF/multilayer urban canopy model and local climate zones. *Urban Clim.* **2020**, *34*, 100714. [CrossRef]
5. D'Ostuni, M.; Zaffi, L.; Appolloni, E.; Orsini, F. Understanding the complexities of Building-Integrated Agriculture. Can food shape the future built environment. *Futures* **2022**, *144*, 103061. [CrossRef]
6. Vujovic, S.; Haddad, B.; Karaky, H.; Sebaibi, N.; Boutouil, M. Urban Heat Island: Causes, Consequences, and Mitigation Measures with Emphasis on Reflective and Permeable Pavements. *CivilEng* **2021**, *2*, 459–484. [CrossRef]
7. Marsaglia, V. Technological Greenery. Exploring cutting-edge solutions for performant Greenery integration in building envelope design. *Energy Build.* **2024**, *324*, 114920. [CrossRef]
8. Li, H.; Guo, Y.; Zhao, H.; Wang, Y.; Chow, D. Towards automated greenhouse: A state of the art review on greenhouse monitoring methods and technologies based on internet of things. *Comput. Electron. Agric.* **2021**, *191*, 106558. [CrossRef]
9. Layher Allround Scaffolding Catalogue 2021/2022 Layher the Scaffold System. Available online: https://www.layher.co.nz/brochures-catalogues-downloads/ (accessed on 4 February 2023).
10. William, Y.E.; An, H.; Chien, S.-C.; Soh, C.B.; Ang, B.T.W.; Ishida, T.; Kobayashi, H.; Tan, D.; Tay, R.H.S. Urban-Metabolic Farming Modules on Rooftops for Eco-Resilient Farmscape. *Sustainability* **2022**, *14*, 16885. [CrossRef]
11. Garland, K.F.; Burnett, S.E.; Stack, L.B.; Zhang, D. Minimum Daily Light Integral for Growing High-quality Coleus. *HortTechnology* **2010**, *20*, 929–933. [CrossRef]
12. Çaylı, A.; Baytorun, A.N. Analysis of climate and vapor pressure deficit (VPD) in a heated multi-span plastic greenhouse. *J. Anim. Plant Sci.* **2021**, *31*, 1632–1644. [CrossRef]
13. Preger, J.J.; Ling, P.P. Greenhouse Condensation Control—Understanding and Using Vapor Pressure Deficit (VPD). In Proceedings of the 2000 ASAE Annual International Meeting, Technical Papers: Engineering Solutions for a New Century, Milwaukee, WI, USA, 9–12 July 2000; Volume 2, pp. 5273–5287.
14. Arve, L.E.; Kruse, O.M.O.; Tanino, K.K.; Olsen, J.E.; Futsæther, C.; Torre, S. Daily changes in VPD during leaf development in high air humidity increase the stomatal responsiveness to darkness and dry air. *J. Plant Physiol.* **2017**, *211*, 63–69. [CrossRef]
15. Ang, B.T.W.; Fong, Y.M.; Soh, C.B.; Chien, S.-C.; An, H.; Tay, R.H.S. Passive Infrared-to-Visible-Light Upconversion Using NaYF4:Yb,Er Nanoparticle Films for Greenhouse Façades. *ACS Appl. Nano Mater.* **2024**, *7*, 18851–18860. [CrossRef]
16. Vinukonda, A.; Bolledla, N.; Jadi, R.K.; Chinthala, R.; Devadasu, V.R. Synthesis of nanoparticles using advanced techniques. *Next Nanotechnol.* **2025**, *8*, 100169. [CrossRef]
17. Sinclair, T.R.; Devi, J.; Shekoofa, A.; Choudhary, S.; Sadok, W.; Vadez, V.; Riar, M.; Rufty, T. Limited-transpiration response to high vapor pressure deficit in crop species. *Plant Sci.* **2017**, *260*, 109–118. [CrossRef] [PubMed]

18. Inoue, T.; Sunaga, M.; Ito, M.; Yuchen, Q.; Matsushima, Y.; Sakoda, K.; Yamori, W. Minimizing VPD Fluctuations Maintains Higher Stomatal Conductance and Photosynthesis, Resulting in Improvement of Plant Growth in Lettuce. *Front. Plant Sci.* **2021**, *12*, 646144. [CrossRef] [PubMed]
19. Noh, H.; Lee, J. The Effect of Vapor Pressure Deficit Regulation on the Growth of Tomato Plants Grown in Different Planting Environments. *Appl. Sci.* **2022**, *12*, 3667. [CrossRef]
20. Shen, L.; Yin, X. Solar spectral management for natural photosynthesis: From photonics designs to potential applications. *Nano Converg.* **2022**, *9*, 36. [CrossRef] [PubMed]
21. Yang, C.-F.; Wang, C.-H.; Ke, P.-X.; Meen, T.-H.; Lai, K.-K. Development and Fabrication of a Multi-Layer Planar Solar Light Absorber Achieving High Absorptivity and Ultra-Wideband Response from Visible Light to Infrared. *Nanomaterials* **2024**, *14*, 930. [CrossRef] [PubMed]